

Alotaibi, Sorour; Alotaibi, Fahad; Ibrahim, Osama M.

Article

Solar-assisted steam power plant retrofitted with regenerative system using Parabolic Trough Solar Collectors

Energy Reports

Provided in Cooperation with:

Elsevier

Suggested Citation: Alotaibi, Sorour; Alotaibi, Fahad; Ibrahim, Osama M. (2020) : Solar-assisted steam power plant retrofitted with regenerative system using Parabolic Trough Solar Collectors, Energy Reports, ISSN 2352-4847, Elsevier, Amsterdam, Vol. 6, pp. 124-133, <https://doi.org/10.1016/j.egy.2019.12.019>

This Version is available at:

<https://hdl.handle.net/10419/244019>

Standard-Nutzungsbedingungen:

Die Dokumente auf EconStor dürfen zu eigenen wissenschaftlichen Zwecken und zum Privatgebrauch gespeichert und kopiert werden.

Sie dürfen die Dokumente nicht für öffentliche oder kommerzielle Zwecke vervielfältigen, öffentlich ausstellen, öffentlich zugänglich machen, vertreiben oder anderweitig nutzen.

Sofern die Verfasser die Dokumente unter Open-Content-Lizenzen (insbesondere CC-Lizenzen) zur Verfügung gestellt haben sollten, gelten abweichend von diesen Nutzungsbedingungen die in der dort genannten Lizenz gewährten Nutzungsrechte.

Terms of use:

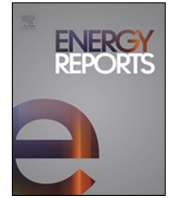
Documents in EconStor may be saved and copied for your personal and scholarly purposes.

You are not to copy documents for public or commercial purposes, to exhibit the documents publicly, to make them publicly available on the internet, or to distribute or otherwise use the documents in public.

If the documents have been made available under an Open Content Licence (especially Creative Commons Licences), you may exercise further usage rights as specified in the indicated licence.



<https://creativecommons.org/licenses/by-nc-nd/4.0/>



Research paper

Solar-assisted steam power plant retrofitted with regenerative system using Parabolic Trough Solar Collectors



Sorour Alotaibi*, Fahad Alotaibi, Osama M. Ibrahim

Department of Mechanical Engineering, College of Engineering and Petroleum, Kuwait University, P.O. Box 5969, Safat 13060, Kuwait

ARTICLE INFO

Article history:

Received 10 June 2019

Received in revised form 29 September 2019

Accepted 19 December 2019

Available online xxxx

Keywords:

Steam power plants
Solar-assisted
Regenerative system

ABSTRACT

This work investigates the performance of a conventional steam power plant retrofitted with a solar-assisted regenerative system using Parabolic Trough Solar Collectors (PTC). The solar collectors were used to compensate for the effect of removing Low-Pressure (LP) turbine extractions without changing other elements of a 300 MW power plant unit during peak load operations. The steam power plant, located in Kuwait, receives high levels of solar irradiation. Modeling of the solar-assisted regenerative system using PTC is simulated for Kuwait's weather conditions. Results of the system analysis show that removing the LP turbine extractions enhanced the performance of the steam power plant by 9.8 MW, with an optimum PTC aperture area equal to 25,850 m². A techno-economic analysis was used to estimate the Levelized Cost of Energy (LCOE). Compared to an equivalent photovoltaic solar plant, the optimum aperture area and LCOE for the PTC solar plant were found to be less by 45% and 44%, respectively. When compared to an equivalent conventional steam turbine, the solar-assisted steam power plant decreased cost by 56% over the lifecycle of 25-years.

© 2019 The Authors. Published by Elsevier Ltd. This is an open access article under the CC BY license (<http://creativecommons.org/licenses/by/4.0/>).

1. Introduction

In 2014, according to the World Bank's data and research, Kuwait was considered seventh in the world in consuming electricity per capita (15,591 kWh per capita) (Worldbank Data, 2014). This high demand for electrical power is being pushed by high economic growth and increasing population. Electricity consumption is growing rapidly in Kuwait, as well as in the other countries in its region. In 2016, an estimation was presented by Kuwait's Ministry of Electricity and Water (Kuwait-MEW) stating that the demand for power in 2030 would be 30,000 MW, with a per capita consumption of 25,350 kWh (Ministry of Electricity and Water of Kuwait, 2017). This last figure represents a five-fold increase in per capita consumption in 40 years. This continuous increase demand for electricity will force Kuwait to build more power plants, but conventional power plants are major oil consumers. The consumption of these power plants would reach more than 26% of Kuwait's total oil production by 2020 (Alotaibi, 2011). Currently, Kuwait is one of the highest emitters of carbon dioxide (CO₂) per capita in the world (31 metric tons per capita), most of which comes from power plants. Building new conventional power plants is not an easy option due to the long execution time required and the related environmental impacts. Therefore, growing interest is being directed toward solar energy.

Kuwait and some parts of the Middle East have significant potential areas for concentrating solar energy, at an annual solar irradiance higher than 2300 kWh/m². Renewable sources of energy have no direct release of emissions; therefore, solar energy is regarded as having a high potential for addressing environmental issues resulting from the combustion of fossil fuels. At the Umm Gudair oil field, Kuwait has started its first solar power plant – a landmark for the country – to diversify its energy resources and meet rapidly rising demands. Kuwait-MEW is also planning a solar energy power plant, “Shaqaya”, with solar and wind projects of 70 MW (Haug, 2014).

Repowering an existing power plant is considered a solution for increasing its efficiency. The process of “repowering” transforms an old power plant to heighten its capacity and efficiency levels. Consequently, repowered plants are characterized by higher power outputs and less specific CO₂ emissions. It is usually performed on an existing steam cycle, built decades ago, by integrating one or more steam/gas turbines into the cycle. Around the globe, several commercial solar hybrid power plants have been commissioned in the last few years. Among these is the first world's hybrid solar and coal power station outside Palisade, Colorado, USA, Mills (2017). This solar-assisted power plant consists of a series of Parabolic Trough Solar Collectors (PTC) integrated with a coal-fired steam power plant. The solar energy heats circulating oil to about 300 °C. The heated oil is then fed into a heat exchanger, where the heat is transferred to the water – heating it to around 200 °C – before it enters the boiler.

* Corresponding author.

E-mail address: sr.alotaibi@ku.edu.kw (S. Alotaibi).

Having hotter water entering the boiler means less fuel is needed to heat the water and produce the steam that turns the turbine to generate electricity. Similarly, the Bukuzindu Hybrid Solar and Thermal Power Station is a 1.6 MW hybrid solar and diesel fuel-fired thermal power plant in Uganda. The hybrid power station has a 0.6 MW solar energy component and a 1.0 MW diesel fuel-fired thermal component. More recent operational hybrid projects include Liddell power plant, and Kogan Creek power station in Australia, and Sundt solar boost project in the USA. At Liddell power plant, the existing 2000 MWe is assisted by 9 MWth solar energy to produce steam at 270 °C and 44 bars which also resulted in cutting the greenhouse gas emissions by approximately 5000 tons per year (Kaushik and Sairam, 2017). Kogan Creek, Solar upgrade project, is considered the world's largest solar integration with a coal-fired power plant. In this project, the solar addition of 44 MW will empower the coal power station of 750 MW to produce steam at 370 °C and 60 bars (AREVA, 2016). More existing operational projects, with their total and solar contributions to power, can be found in Baharoonah et al. (2015).

The integration of solar power with fossil fuel power plants can be explored as a feasible option for cleaner and cheaper generation of power. Cakici et al. (2017) showed that integrating the organic Rankine cycle (ORC) with PTC is a better option than the stand-alone ORC system for obtaining higher net power outputs. Mokheimer et al. (2014) performed a sizing analysis of PTC integrated with steam and binary vapor cycles; the optimization shows that lowering the mass flow rate of heat transfer fluid (HTF) per each solar collector row, within the range considered, reduces the required number of solar collector rows and, thus, saves cost.

Hybridizing an existing thermal power plant with a Concentrated Solar Plant (CSP) has raised the attention of researchers in recent decades due to its benefits in performance, low environmental impact, and low cost. Some studies estimate that CSPs are likely to contribute about 7% to global electricity production by 2050, and they will catch up and overtake solar PVs in the near future due to their lower integration costs (Mehrpooya et al., 2017; Poullikkas et al., 2012). In hybridizing a power plant, Kalogirou et al. (1997) concluded that 49% of available solar radiation is used for steam generation, and the remaining radiation is lost, either in the collectors or as thermal losses. There are many ways for increasing efficiency when hybridizing power plants, such as boiler reheating. But based on the literature review, the feedwater heater is considered the most developed hybrid concept, including a CSP field with a direct steam generation (Suojanen et al., 2017). Cakici et al. (2017) utilized a CSP, with its solar-geothermal heat exchanger just prior to the turbine, to increase its inlet temperature (considering the maximum temperature constraints of the turbine). Hence, power output performance increased by 11%. Mehrpooya et al. (2017) investigated the integration of CSPs into an ORC by dividing the boiler into three heat exchangers (economizer, evaporator, and superheater), which exchange heat with the CSP. Poullikkas et al. (2012) optimized the sizing of a steam turbine for a given CSP while maintaining a constant inlet turbine temperature. They concluded that, by increasing the capacity of the plant, the turbine's steam inlet pressure at which maximum efficiency can be obtained increased up to a capacity of 50 MW and remained constant at 140 bar. It was found that an immediate improvement of 5%–6% in coal consumption can be achieved by substituting the turbine bleed stream by solar-assisted feed-water heater (You and Hu, 1999). Qin et al. (2011) have shown that solar aided power generation is an efficient way to use solar energy in the low and medium temperature range for power generation by replacing turbine's bleed steams to feedwater heaters with solar energy. Four cases were suggested to bleed steam from turbines at 260 °C, 200 °C, 160, and 100 °C.

Bakos and Tsehelidou (2013) have simulated the operation of the 300 MW power plant integrated with 27 MW PTC solar field. The solar field was designed to supply the highest feedwater heater with the desired temperature of 390 °C. The power plant performance, fuel consumption, and CO₂ emissions showed improvement. Boukeliia et al. (2015) have conducted energy, exergy, economic, and environment (4E) comparative investigation of eight distinct configurations of PTC power plants with two different working fluids, with and without thermal energy storage or/and backup fuel system. Their results have indicated that the configurations based on molten salt are better in terms of environmental and economic parameters.

According to previous studies, the best integration of a CSP plant with the steam cycle of power plants depends mainly on current power plant conditions. Most of the previous studies mentioned have integrated solar plants as a replacement for the feedwater preheater or the boiler itself. However, technically and practically, for an existing power plant, it would be better not to change or replace the feedwater preheaters or the existing boiler in most cases. Replacing the extraction only with feed water from a steam turbine equipped with a CSP can increase the power of the plants without affecting the other steam cycle elements.

In this study, we suggest modifying an existing power plant (Az-Zour South) in Kuwait to increase its efficiency by replacing steam extractions from the turbine with a CSP. This modification will be evaluated and studied.

2. Az-Zour south power plant description

Most of the old power plants in Kuwait are combined power desalination plants with extraction-condensing steam turbines. Recently, more gas turbines and combined cycles have been introduced in the system of power generation. Due to harsh weather conditions and the long summer season, which extends from April to October, most of the power plants work on full loads to supply power and desalted water. Az-Zour South power plant is commissioned in 1988 and located in the southern region of Kuwait. It consists of eight power plant units, each with a rated electrical power output of 300 MW, resulting in a maximum capacity of 2400 MW. During the summer season, from April to October, these steam power units usually are working near their maximum capacity during peak hours with a drop between 5%–10% at off-peak hours during night. The boiler is using natural gas as a primary fuel and fuel oil (gas oil) as a back-up fuel. The number of operating hours per year varies from 5800 to 7750. The total output power per year varies from 1,119,320 MWh to 1,447,191 MWh. A flow diagram of one of these eight units is shown in Fig. 1, which is used as a reference in this study. The cycle uses regenerative feedwater heaters, five closed and one open. Steam is extracted from the eight turbines and sent to these feedwater heaters to improve the thermal efficiency and to avoid thermal shock in the boiler. Steam is also extracted to operate desalting units. Pressure, temperature, enthalpy, and mass flow rate data at each thermodynamic state of the steam cycle, for an actual summer operation producing 273 MW of electricity, are given in Table 1.

The steam turbines cycle in Az-Zour South power plant consists of HP, IP, and LP turbines. Each type of turbine has different extraction properties for water heading to the deaerators and feedwater heaters for maintaining the boiler load. Isolating one or two extractions from a turbine is enough to maintain minimum changes to the steam turbine cycle and not to exceed the turbine's maximum allowable power output because overloading the turbine blades can cause failure. Reference to Fig. 1, there are six extractions in the steam turbine plant—five for the five feedwater heaters and one for the deaerator. The extraction with

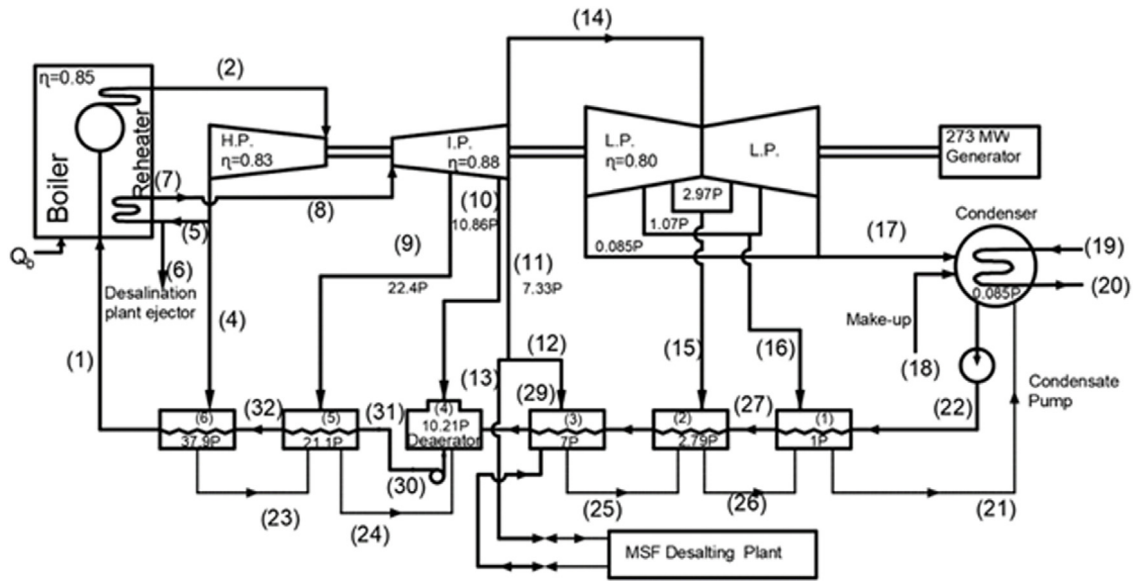


Fig. 1. Flow diagram of a steam power unit of Az-Zour South cogeneration power plant in Kuwait (Ministry of Electricity and Water of Kuwait, 2017).

Table 1
Thermodynamic properties and mass flow rate data, for an actual operation producing 273 MW of electricity, of the steam cycle shown in Fig. 1 (Ministry of Electricity and Water of Kuwait, 2017).

State	\dot{m} (kg/s)	T (°C)	P (bars)	i (kJ/kg)	Node	\dot{m} (kg/s)	T (°C)	P (bars)	i (kJ/kg)
1	261.10	246.1	160.00	1068	17	182.00	43.3	0.085	2347
2	261.10	535	139.00	3420	18	0	–	–	141.6
3	261.10	355.8	39.60	3107	19	9299	25.0	–	–
4	17.84	355.8	39.60	3107	20	9299	35.0	–	–
5	243.30	355.8	39.60	3107	21	40.56	50.0	0.123	209.3
6	0	–	–	–	22	222.50	43.3	0.087	181.3
7	243.30	535	39.60	3107	23	17.84	217.6	37.90	932.9
8	243.30	535	36.70	3529	24	30.46	187.8	21.10	798.2
9	12.62	462.8	22.40	3383	25	13.20	131.1	7.00	551.4
10	8.12	362.7	10.86	3183	26	24.20	102.0	2.79	427.6
11	13.20	313.9	7.33	3087	27	222.50	95.3	1.00	399.3
12	13.20	313.9	7.33	3087	28	222.50	126.6	2.79	531.9
13	0	–	–	3086	29	222.50	151.1	7.00	637.4
14	209.30	313.1	7.19	2891	30	261.10	167.5	10.21	708.5
15	11.00	212.7	2.97	2705	31	261.10	184.3	11.05	850.3
16	16.36	114.8	1.07	2347	32	261.10	214.1	160.00	829.1

the highest mass flow rate is State 4, and the extraction with the second-highest mass flow rate is State 16. The temperature in State 4 is too high when compared with the temperature in States 15 and 16, also having a near atmospheric pressure of 1.07 and 2.97 bars, respectively. Therefore, in this project, the extractions from the LP turbine to the first and second feedwater heaters will be removed and substituted with the solar plant. States 15 and 16 were selected due to their reasonable mass flow rates, temperature, and pressure, which can easily be supplied by solar energy.

A feedwater heater is used in power plants as a preheater for the boiler. The source of heat is steam bled from the turbines, and its purpose is to enhance the cycle's thermal efficiency by reheating the water before it enters the boiler, thereby avoiding thermal shock inside the boiler. Feedwater heaters can be divided into two types—open and closed. In an open feedwater heater, bled steam coming from the turbine will be mixed with the feed water in the heater or the heat exchanger. A mixture of bled steam and feed water will leave the feedwater heater or heat exchanger at the same temperature. The process is controlled such that discharge from the feedwater heater will be in the saturated liquid phase—i.e., State 27, as shown in Fig. 2 and listed in Table 1. In a closed feedwater heater, the feed water will flow through tubes of the heat exchanger (shell and tube heat exchanger) and

bled steam will flow within the shell over the surface of the heat exchanger's tubes. The Drain Cooling Approach (DCA), defined as the difference between drain outlet temperature and feedwater heater inlet temperature, is equal to 6.7 °C in the first and second feedwater heaters. The Terminal Temperature Differences (TTD), defined as the difference between the saturation temperature of the extracted steam and the feedwater heater exit temperature, is equal to 6.2 °C and 6.8 °C in the first and second feedwater heaters respectively. Also, the temperature rise which is defined as the difference between inlet and outlet temperatures across the feedwater heater, is equal to 52 °C and 31.3 °C in the first and second feedwater heater, respectively.

In this suggested modification of the cycle, the lines of extracted steam will head to closed feedwater heaters, shown in Fig. 2, and they can be modeled with energy balance as follows:

$$\dot{m}_{22}(i_{27} - i_{22}) = \dot{m}_{16}i_{16} + \dot{m}_{26}i_{26} - \dot{m}_{21}i_{21} + \dot{Q}_{loss} \quad (1)$$

where \dot{Q}_{loss} is the heat loss in the shell and tube heat exchanger.

3. Solar plant model

In this section, a solar plant will be designed and sized, according to Kuwait's weather conditions. This project focused on CSP system design, cycle parameters, and cycle efficiency. As

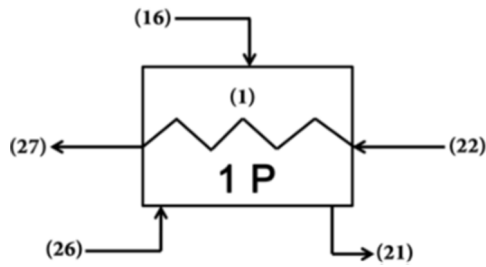


Fig. 2. Closed feedwater preheater.

mentioned in the introduction, Kuwait is within an area of the significant potential for concentrating solar power, at an annual solar irradiance of higher than 2300 kWh/m²/y. Solar irradiation depends on many factors, such as location, local time, solar angles, and weather conditions. The American Society of Heating, Refrigerating and Air-Conditioning Engineers (ASHRAE) developed constant parameters by experimentally measuring solar irradiation throughout the year, and, hence, models are developed to predict solar irradiation at given conditions. The ASHRAE clear sky model is commonly used as a basic tool to estimate solar irradiation. This model, however, was developed for the atmospheric conditions of the USA, which are quite different from weather conditions in Kuwait. [Alsadi and Nassar \(2016\)](#) revised all the parameters of the ASHRAE model according to the atmospheric conditions of Middle East countries in an attempt to improve the model's accuracy, which was used in this study.

3.1. Concentrated solar power (CSP)

CSP uses mirrors or lenses to concentrate a large area of sunlight onto a small area to heat a fluid in a collector at high temperature. Unlike photovoltaic (PV) cells or flat plate solar thermal collectors, the CSP energy conversion process consists of three parts: (1) the concentration of solar energy, (2) the conversion of solar energy into useful thermal energy, and (3) the conversion of heat into electricity. The conversion of heat into electricity is generally realized by a conventional steam turbine. There are four available CSP technologies: PTC, linear Fresnel collectors, solar towers, and parabolic dishes. PTC technology is the most developed and commercialized in many parts of the world. Currently, about 90% of CSP power plants worldwide use PTC technology ([Shahin et al., 2016](#)). PTC, as shown in [Fig. 3](#), consists of mirrors, tube heat receivers, and structural support. The parabolic mirrors are formed by a flat sheet of reflective material, manufactured in a parabolic shape, which concentrates directed sunlight onto a focal receiver line. The receiver line is made up of an absorber tube inside a glass envelope. Heat transfer fluid is circulated through the receiver tubes to absorb the most solar energy and exchange it in the steam generator or thermal energy storage. Most existing commercial PTC use synthetic oils as the circulated heat transfer fluid inside the receiver, which can operate up to 400 °C.

The type of collector selected in this research is the LS-3 collector, shown in [Fig. 3](#). This collector has been chosen because it is most common and well-known collector design in solar power generating plants. It has larger dimensions than the LS-1 and LS-2 collectors, and its size has proven performance, especially in larger CSP plants. It operates on a horizontal north–south axis and tracks the sun from east to west. The receiver tube is made of stainless steel and is coated with a selective coating to increase its absorptivity to incoming radiation. The receiver is also enclosed with a glass evacuated tube of 66 mm inner diameter to reduce convective heat losses. The LS-3 Solar collector specifications are detailed in [Table 2](#).

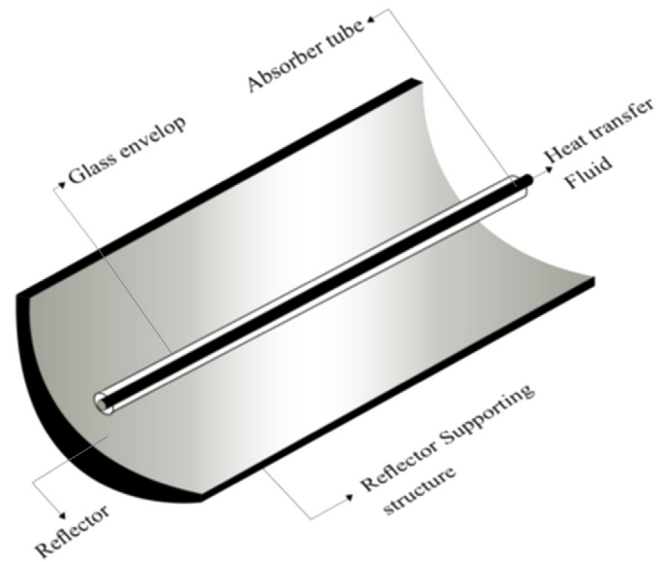


Fig. 3. Parabolic trough solar collector (PTC) of LS-3 type.

Table 2
LS-3 Solar collector specifications ([Shahin et al., 2016](#)).

Parameter	Symbol	Value
Single collector width × length	$W_w \times L$	5.77 m × 12 m
Receiver inner and outer diameter	$D_{r,i}, D_{r,o}$	0.066 m, 0.07 m
Cover inner and outer diameter	$D_{c,i}, D_{c,o}$	0.115 m, 0.121 m
Emissance of the cover and receiver	$\epsilon_{cv}, \epsilon_r$	0.86, 0.15
Reflectance of the mirror	ρ_c	0.93
Intercept factor	γ_i	0.93
Transmittance of the glass cover	τ	0.94
Absorbance of the receiver	α	0.94
Incidence angle modifier	K_r	1
Mass flow rate in the receiver	m_o	0.8 kg/s

3.2. Absorber design and efficiency

In this section, modeling of the LS-3 will be carried out to obtain the useful heat rate of the collector, as well as its thermal efficiency. Several researchers studied and proposed heat transfer models for PTC, e.g., [Patnode \(2006\)](#), [Clark \(1982\)](#), [Forristall \(2003\)](#), [Padilla et al. \(2011\)](#) and [Duffie and Beckman \(2013\)](#). A detailed one-dimensional heat transfer model of PTC was proposed by [Padilla et al. \(2011\)](#). In this current work, however, the optical efficiency η of the LS-3 PTC was calculated from a simple model described in [Duffie and Beckman \(2013\)](#) as follows:

$$\eta = \rho_c \gamma_i \tau \alpha K_r \quad (2)$$

where K_r is the incidence angle modifier, which can be defined as the ratio of the optical solar field efficiency at a given incidence angle to the optical solar field efficiency. Gaul et al. studied the incidence angle modifier K_r for several, commercially available, parabolic trough collectors. From test data of this tracking system, K_r was approximated to unity which is quite acceptable for use in calculation of long-term energy delivery ([Gaul and Rabl, 1980](#)). The heat absorbed by the receiver can be calculated as:

$$S = G_t \eta \quad (3)$$

where G_t is total irradiation and η is the optical efficiency. The area geometry of the parabolic trough is given by:

$$A_{ap} = (W - D_{r,o})L \quad (4)$$

$$A_r = \pi D_{r,o}L \quad (5)$$

$$A_{ri} = \pi D_{ri}L \quad (6)$$

$$A_{cv} = \pi D_{cv} L \quad (7)$$

where A_{ap} is the aperture area; A_r is the surface area of the receiver; A_{ri} is the inner surface area of the receiver; and A_{cv} is the surface area of the cover. The correlation for the specific heat of the heat transfer fluid (Therminol-VP1) can be found in [Eastman Chemical Company \(0000\)](#):

$$C_p = 0.002414T_o + 59591 \times 10^{-6}T_o^2 - 29879 \times 10^{-8} \times T_o^3 + 44172 \times 10^{-11}T_o^4 + 1498 \quad (8)$$

where T_o is the oil temperature in degrees Celsius. The efficiency factor F_1 of the collector is the ratio of the overall heat loss coefficient from the surroundings to the fluid U_o and the solar collector heat loss coefficient U_L ,

$$F_1 = \frac{U_o}{U_L} \quad (9)$$

Hence, the heat removal factor,

$$F_R = \frac{\dot{m}_o C_{p,avg}}{A_r U_L} \left[1 - e^{-\frac{A_r U_L F_1}{\dot{m}_o C_{p,avg}}} \right] \quad (10)$$

where the $C_{p,avg}$ is the average specific heat of the oil between inlet and outlet temperatures. The radiation heat coefficients are equal to:

$$h_{R,a,cv} = \varepsilon_{cv} \sigma (T_{cv} + T_a) (T_{cv}^2 + T_a^2) \quad (11)$$

$$h_{R,r,cv} = \sigma (T_{cv} + T_{o,avg}) \left[\frac{T_{cv}^2 + T_{o,avg}^2}{\frac{1}{\varepsilon_r} + \frac{A_r}{A_{cv}} \left(\frac{1}{\varepsilon_{cv}} - 1 \right)} \right] \quad (12)$$

where σ is the Stefan–Boltzmann constant ($\sigma = 5.67 \times 10^{-8} \text{ W m}^2 \text{ K}^{-4}$); $h_{R,a,cv}$ is the radiation heat coefficient between the ambient conditions and the receiver cover; $h_{R,r,cv}$ is the radiation heat coefficient between the receiver and the cover; and ε_r and ε_{cv} are the emittance of the receiver and cover, respectively. For the heat transfer between the absorber cover and the ambient air, the Reynolds and Nusselt numbers are:

$$Re_a = \frac{V_a D_{ro}}{\nu_a} \quad (13)$$

$$Nu_a = 0.3Re_a^{0.6} \quad (14)$$

Therefore, the convection heat coefficient between the cover and the ambient conditions is;

$$h_{cv,a} = \frac{Nu_a k_a}{D_c} \quad (15)$$

And the solar collector heat loss coefficient can be written as,

$$U_L = \left[\frac{A_r}{(h_{cv,a} + h_{R,a,cv} A_{cv})} + \frac{1}{h_{R,r,cv}} \right]^{-1} \quad (16)$$

The heat transfer between the absorber cover and receiver can be written as:

$$h_{cv,o} = \frac{Nu_o k_o}{D_{ri}} \quad (17)$$

The temperature of the cover T_c is given by:

$$T_c = \frac{h_{R,r,cv} T_{o,avg} + \frac{A_{cv}}{A_r} T_o (h_{cv,a} + h_{R,a,cv})}{h_{R,r,cv} + \frac{A_{cv}}{A_r} (h_{cv,a} + h_{R,a,cv})} \quad (18)$$

The overall heat coefficient from the surroundings to the fluid:

$$U_o = \left[\frac{1}{U_L} + \frac{D_{ro}}{h_{cv,r} D_{ri}} + \frac{D_{ro}}{2k_o} \ln \left(\frac{D_{ro}}{D_{ri}} \right) \right]^{-1} \quad (19)$$

Table 3

Solar plant input operating conditions ([Shahin et al., 2016](#)).

Parameter	Symbol	Value
Ambient temperature and velocity	T_a V_a	298 K, 5 m/s
Total solar beam radiation	I_t	670.6 W/m ²
Therminol-VP1 oil density	ρ_o	1060 kg/m ³
Thermal conductivity of air	k_a	0.024 W/m K
Thermal conductivity of oil	k_o	0.096 W/m K
Kinematic viscosity of oil	ν_o	$9.9 \times 10^{-7} \text{ m}^2/\text{s}$
Temperature at receiver output and input	T_{ro}, T_{ri}	663 K, 330 K

Hence, the useful energy rate from the collector:

$$\dot{Q}_u = A_{ap} F_R \left[S - \frac{A_r}{A_{ap}} U_L (T_{ri} - T_a) \right] \quad (20)$$

Also, it can be written as:

$$\dot{Q}_u = \dot{Q}_{solar} - \dot{Q}_{loss} \quad (21)$$

where,

$$\dot{Q}_{solar} = A_{ap} F_R S \quad (22)$$

$$\dot{Q}_{loss} = F_R A_r U_L (T_{ri} - T_a) \quad (23)$$

where \dot{Q}_{solar} is the heat gained from solar energy in the collector, and \dot{Q}_{loss} is the total heat loss from the collector in all modes. Adding useful energy from all collectors, the total will be:

$$\dot{Q}_{u,total} = \dot{Q}_u N_C \quad (24)$$

where, N_C is the total number of collectors.

3.3. Solar plant efficiency

Solar plants should be designed to supply at least the required thermal energy or more. Considering this condition will lead to maintaining $\dot{Q}_{u,total} \geq \dot{Q}_{sol,req}$. This must be applied to maintain the load in the boiler, and it will define the collector thermal efficiency as follows,

$$\eta_{c,th} = \frac{\dot{Q}_u}{G_t A_{ap}} \quad (25)$$

where G_t is the average total irradiation per day calculated at the plant location. Selected properties and input operating conditions of the solar plant are shown in [Table 3](#).

4. Integrated power cycle model

Az-Zour South cogeneration power plant, integrated with a solar plant, is shown in [Fig. 4](#) with the associated mass flow rates and temperatures of the oil and steam. The solar plant consists of parabolic trough collectors and a steam generator. The steam generator is a heat exchanger, which exchanges heat between the heat transfer fluid (therminol-VP1) and steam, as shown in [Fig. 4](#). The therminol-VP1 must heat the steam to thermodynamic properties similar to the original properties when extracted from the LP turbine to the feedwater heater (States 15 and 16). Assuming the heat exchanger has an efficiency of $\eta_{HE} = 85\%$, then we have

$$\dot{Q}_{sol,req} = \dot{m}_{o,total} C_{p,avg} (T_{ro} - T_{ri}) \quad (26)$$

$$\dot{Q}_{st,req} = (\dot{m}_{16} i_{16} + \dot{m}_{15} i_{15}) - \dot{m}_{17} i_{17} \quad (27)$$

$$\dot{Q}_{sol,req} = \dot{Q}_{st,req} / 0.85 \quad (28)$$

where $\dot{m}_{o,total}$ is the total oil mass flow rate, $\dot{Q}_{st,req}$ is the required steam energy, and T_{ri}, T_{ro} are the inlet and out oil temperatures respectively; $\dot{Q}_{sol,req}$ is the required energy from the solar field.

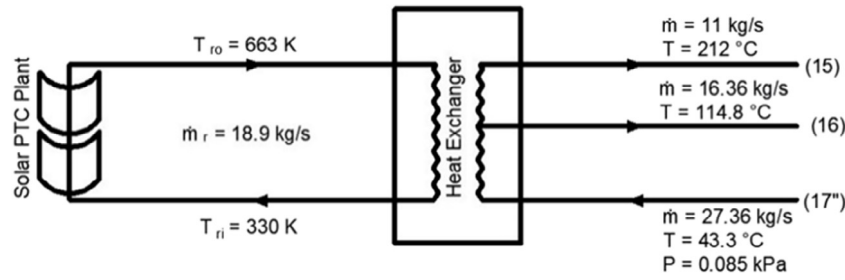


Fig. 4. Steam and oil flow in the solar plant and heat exchanger.

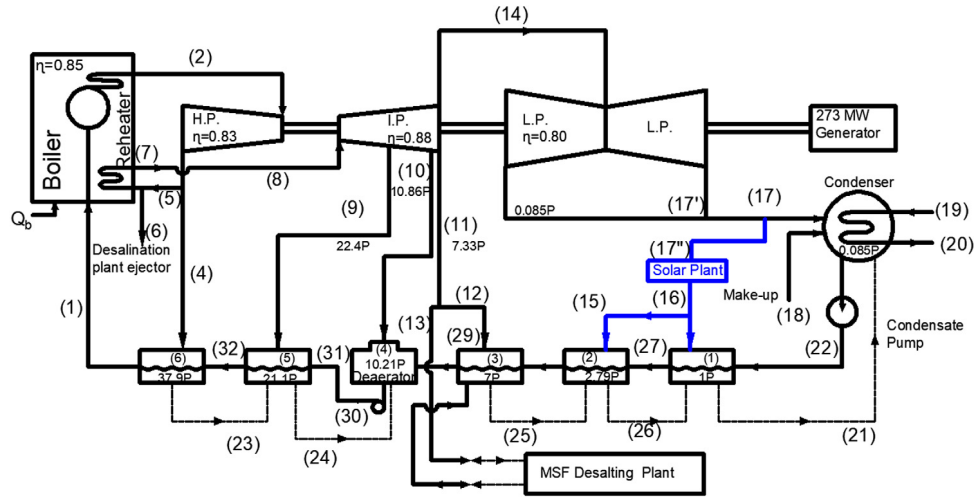


Fig. 5. Flow diagram of a modified steam power unit integrated with the solar plant producing 282.8 MW (Worldbank Data, 2014).

Fig. 5 shows the hybridized power plant with the solar field, which increased the power output to 282.8 MW. The steam extraction from the LP turbine at States 15 and 16 in the original power plant have now been removed. As a result, more steam flow rates will pass through the turbine, providing more power. The extraction for the solar plant will now be taken at State 17, after the LP turbine, with lower energy grade, as shown in Fig. 4. This saving in steam extraction will cause the power output from the cycle to increase by 9.8 MW. The CSP plant is formed by a solar field of PTC and a heat exchanger, in which thermoinoil-VP1 heats the steam coming from State 17 to reach a similar thermodynamic property as States 15 and 16 and maintain the same boiler load.

4.1. Cycle efficiencies

The performance of the steam turbine cycle will be measured from the cycle efficiency and thermal efficiency. The heat input required from burning the fuel in the boiler can be written as:

$$\dot{Q}_b = \dot{Q}_{th,b} / \eta_b \quad (29)$$

And the thermal heat input to the steam in the boiler is,

$$\dot{Q}_{th,b} = \dot{m}_1(i_2 - i_1) \quad (30)$$

where η_b is the boiler efficiency, and $\dot{Q}_{th,b}$ is the thermal heat input to the steam. The HP, IP, and LP turbines' power outputs are defined as:

$$\dot{W}_{HP} = \eta_{HP} \dot{m}_2(i_2 - i_3) \quad (31)$$

$$\dot{W}_{IP} = \eta_{IP} [\dot{m}_8 i_8 - (\dot{m}_9 i_9 + \dot{m}_{10} i_{10} + \dot{m}_{11} i_{11} + \dot{m}_{14} i_{14})] \quad (32)$$

$$\dot{W}_{LP1} = \eta_{LP} [\dot{m}_{14} i_{14} - (\dot{m}_{15} i_{15} + \dot{m}_{16} i_{16} + \dot{m}_{17} i_{17})] \quad (33)$$

where η_{HP} , η_{IP} , and η_{LP} are the HP, IP, and LP turbine efficiencies, respectively. This makes the total power generated from the power plant equal to,

$$\dot{W}_{total} = \dot{W}_{HP} + \dot{W}_{IP} + \dot{W}_{LP,1} \quad (34)$$

The thermal efficiency of the cycle and the thermal efficiency of the power plant are given by:

$$\eta_{cycle} = \dot{W}_{total} / \dot{Q}_b \quad (35)$$

$$\eta_{th} = \dot{W}_{total} / \dot{Q}_{th,b} \quad (36)$$

After isolating the extraction lines (15 and 16) from the LP turbine, the power output from the LP turbine is defined as,

$$\dot{W}_{LP2} = \eta_{LP} [\dot{m}_{14} i_{14} - (\dot{m}_{15} + \dot{m}_{16} + \dot{m}_{17} i_{17})] \quad (37)$$

which leads to new total power and efficiencies.

5. Evaluation of the proposed model

The proposed clean solar energy project will enhance and improve the performance and life of power plants. To show the economic effects of the proposed integrated system, the Levelized Cost of Energy (LCOE) will be considered based on the design conditions in Tables 2 and 3. An optimum solar field, based on LCOE, will be selected first. Then, a comparison between the cost of producing the extra 9.8 MW from the proposed solar plant, a fossil-fuel-powered plant, and a photovoltaic plant will be discussed.

5.1. Levelized Cost of Energy (LCOE)

LCOE is a primary metric for evaluating the cost of electricity generation for the period of a project's life. LCOE includes capital

$$LCOE = \frac{CC \times Y + \sum_{n=1}^n O\&M (1 + j)^n + CostB \times NOB \times n + NOB \times CO_2PB \times CostRM \times n - CostINC \times EngG}{1000 \times 365 \times 24 \times CF \times \sum_{n=1}^n (1 - DG \times n)} \quad (38)$$

Box 1.

cost, operating and maintenance cost, taxes, inflation, interest rates, land cost, incentives, revenues, and net capacity factors. The lowest LCOE defines the best choice. LCOE is equal to the ratio of the total cost over a project's entire lifecycle to the total energy generated. It can be described as Eq. (38) in \$/kWh given in Box 1. where CC is Capital Cost, Y: Recovery factor, O&M: Operation and maintenance over the lifecycle (US\$), j is inflation rate (%), n: Life of power plant in years, Cost B: Cost of oil barrel or equivalent money (US\$) used or saved, NOB: Number of barrels used or saved, CO₂PB: CO₂ generated or saved per barrel of oil (kg/b), CostRM: Cost of removal CO₂ (US\$/kg), PRM: Amount of CO₂ avoided or controlled per kWh (kg_{CO₂}/kWh), CostINC = CostRM × PRM: Cost of incentive provided by the kWh generated or cost of removal CO₂ per kWh (US\$/kWh), EngG: Energy Generated (kWh), CF: Capacity factor, and DG: Degradation factor. These parameters are shown in Table 4. Carbon Oxides (CO₂) is a central part of pollution in the atmosphere. Greenhouse issues guide us to consider the environmental effects of CO₂ from thermal power plants. Removing CO₂ will penalize the efficiency of power plants. The efficiency of plants can be reduced from 40% to 30% with the current technology. CO₂ removing technologies are capital and energy extensive; hence, it will be considered in calculating the LCOE.

These parameters are shown in Table 4. Global warming leads researchers to consider the environmental effects of CO₂ from thermal power plants. However, removing CO₂ will penalize power plant efficiency. The efficiency of plants can be reduced from 40% to 30% with the most current methods. CO₂-removing technologies are also capital and energy extensive, and, hence, they will be considered in calculating LCOE.

In Kuwait, the cost of electricity production in 2018 was 28 Fils/kWh or 28 KWD/MWh, which is equivalent to US\$93.36/MWh, according to the Kuwait-MEW statistics. This number includes fuel prices, production costs, and operating and maintenance costs. Summing up the cost over 25 years, assuming fixed electricity costs for upcoming years, results in 671 Fils/kWh—that is, US\$2.21/kWh. This US\$2.21/kWh is considered the LCOE for the last 25 years. This cost usually includes power generation, transportation, and distribution. For producing the intended 9.8 MW from the solar field, LCOE will first be used to choose the optimum solar area required. Then, it will be used to evaluate and compare the economic aspects between producing this power using an oil-fired steam turbine and using a solar plant over the project's lifecycle. Table 4 shows the input and constant parameters for both cases.

5.2. Oil-fired steam turbine power plant cost

In this section, the above equation will be used to calculate the LCOE for a conventional, oil-fired steam turbine, comparing it with the system presented in this research. Fuel-powered electricity generation plants do not receive any incentives from governments compared to solar plants, mainly due to CO₂ emissions. The cost of crude oil per barrel is kept constant (50 US\$/barrel) in the LCOE evaluation over the power plant's life expectancy. The capital cost is estimated to be US\$ 1200/kW, and the operation and maintenance are estimated to be at 4% from the capital cost plus inflation.

Table 4

LCOE input parameters for both solar and fossil-fuel-powered plants.

Parameter	Value
Number of years	25
Recovery factor, Y	1
Inflation rate, j (%)	3
Capacity factor, CF	0.5
O&M, from capital cost plus inflation, solar and fuel power plant (%)	1.4
Degradation factor, DG (%)	1
Cost of oil barrel or equivalent money, Cost B (US\$)	50
Number of barrels used or saved, NOB (US\$/barrel)	35
Cost RM (US\$/kg of CO ₂)	0.055
CO ₂ per Barrel (kgCO ₂ /barrel)	320
Amount of CO ₂ avoided or controlled per kWh, PRM, (kg _{CO₂} /kWh)	0.93
CostINC = CostRM × PRM (\$/kWh)	0.051
Energy generated, EngG, (9800 kw * 12 h)	117.6 MWh

5.3. Photovoltaics and parabolic trough collector plants cost

The capital cost of renewable energies, such as solar PV plants, is very high compared to conventional steam-powered plants, due to the high installation costs of the solar modules. The National Renewable Energy Laboratory (NREL) has produced annual cost benchmarks since 2009, from the perspective of PV project installers. The type of costs and their value for PV plant projects presented here are taken from the NREL (Fu et al., 2016). The NREL has also developed the solar advisor module (SAM), which is used to predict the cost of a parabolic trough solar plant. The input cost values used in SAM are taken from Kurup and Turchi (2015).

6. Results and discussion

The monthly average total irradiation and the PTC's thermal efficiency throughout the year can be calculated using the procedure described in Duffie and Beckman (2013), and the results are presented in Fig. 6. As shown in this figure, the highest irradiation and thermal efficiency occurred in July (281.6 kWh/m² and 69.6%) and the lowest in January (137.1 kWh/m² and 35.6%).

From the averaged total irradiation during the day (sunrise to sunset) for each month, shown in Fig. 6, and the LS-3 properties and operating conditions of the solar field, shown in Tables 2 and 3, the total aperture area needed each month to provide the required thermal energy of 9.8 MW was found and plotted in Fig. 7.

As shown in Fig. 7, in winter more aperture area is needed than in summer due to lower irradiance. The maximum demand of power from the power plant occurs during summer, especially in July, when the maximum total irradiation is reached, and, hence, a minimum aperture area is required to supply the feedwater heaters with the required energy. A proper aperture area with respect to the full load operation is a fundamental choice. An area that is too large will be partially useless under high solar irradiance values in summer, whereas a small area will mainly be sufficient during the summer months and only partially during the rest of the year. To find the optimum aperture area, LCOE is used, based on the design parameters for each month of

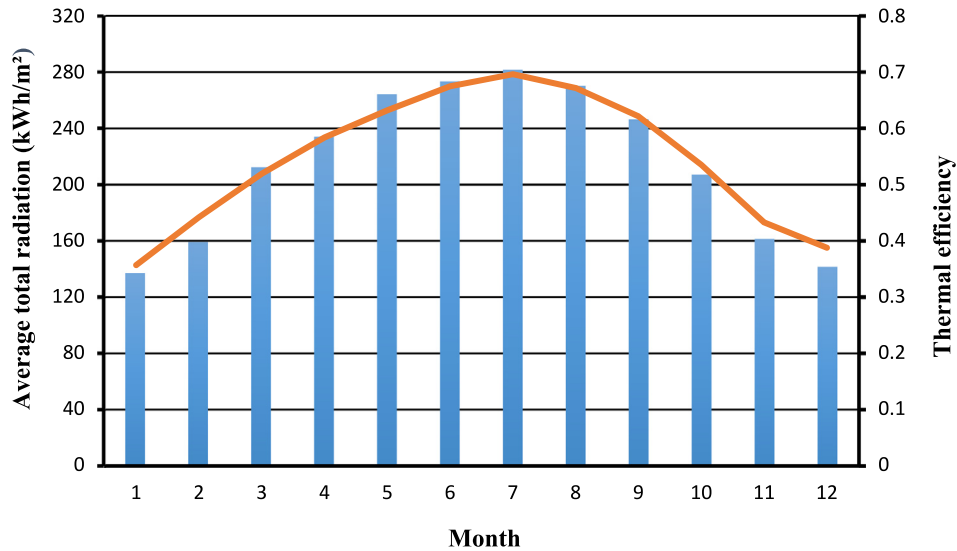


Fig. 6. Distribution of monthly averaged total irradiation and thermal efficiency throughout the year.

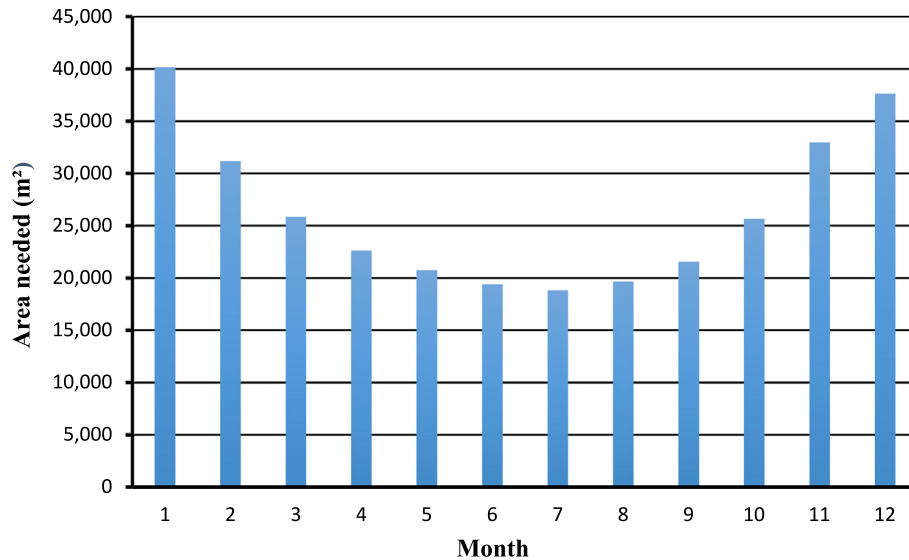


Fig. 7. Total aperture area needed for each month.

the year. Fig. 8 shows the LCOE in each month for the proposed model, based on irradiance and the aperture area required by each month. During summer months, when the irradiance is high, and the required aperture area is small, the energy produced by the aperture area would not be sufficient for the rest of the year. Therefore, the cost of the extra energy needed to supply the necessary 9.8 MW was considered, based on a conventional thermal power plant during the months of insufficient energy. From Fig. 8, the January LCOE equals \$0.175/kWh, corresponding to the maximum aperture area of 40,161 m². The aperture area decreases from January until July, when it reaches its minimum at 18,835 m². On the other hand, the LCOE first decreases, reaching a minimum value of \$0.129/kWh in March and then increases until July at a maximum of \$0.232/kWh. It then begins to decrease again as the cycle continues. Therefore, the optimum aperture area in the year exists in March, corresponding to an aperture area of 25,850 m² and consisting of 378 collectors, each with an aperture area of 69.24 m².

The optical and thermal efficiency of the LS-3 parabolic trough is shown in Table 5 and is within its known performance range. Applying the above results, the performance of the hybridized cycle is shown in Table 6. It is worth mentioning that the thermal efficiency, as shown in Fig. 6, reaches its maximum value in summer and minimum value in winter. It is approximately 69.6% in July and 35.6% January. Despite the high thermal efficiency in summer, the annual average performance, based on LCOE, reveals the optimum design over the life of the project. In this project, March exhibited the optimum aperture area, indicating that the optimum design month does not necessarily have to be the month of highest solar thermal efficiency.

From Table 6, the simulation results reveal an increase of 9.8 MW of total power output when integrating the steam turbine cycle with a solar plant from the LP turbine extractions. The rest of the steam turbine cycle was kept the same, including the boiler load. The cycle and thermal efficiencies showed an increase from the original power plant performance—from 38.6% to 40%,

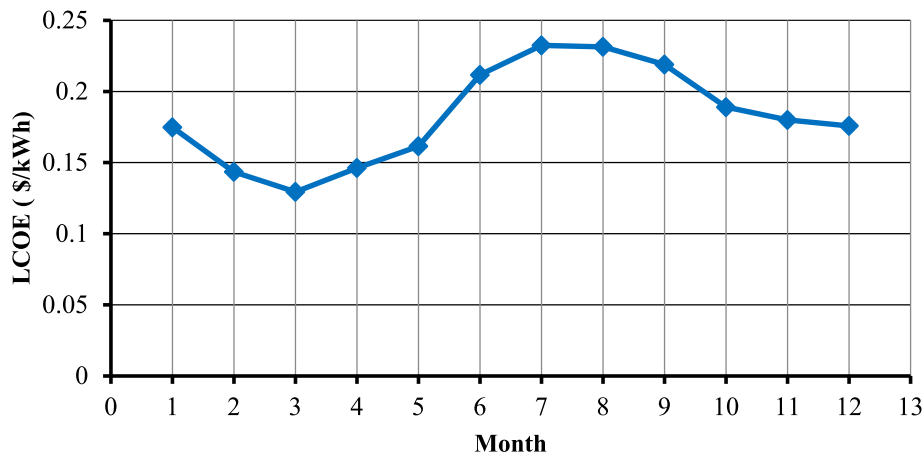


Fig. 8. LCOE of the proposed model for each month.

Table 5

Results of the energy analysis for the parabolic trough collector.

Parameter	Symbol	Value
Heat required for steam from the solar plant heat exchanger	$\dot{Q}_{steam,required}$	11.86 MW
Total heat required from the solar collectors	$\dot{Q}_{solar,required}$	13.80 MW
Total receiver mass flow rate	$\dot{m}_{r,total}$	18.88 kg/s
Total number of collectors	N_c	378
Total needed aperture area on March	A_{needed}	25,853 m ²
Total useful energy rate from the collectors	$\dot{Q}_{u,total}$	13.91 MW
Collector optical and thermal efficiencies (March)	$\eta_r, \eta_{c,th}$	76.5%, 51.9%

Table 6

Performance of Az-Zour South steam turbine cycle.

Parameter	Symbol	Value
Original power plant		
Total power output	$\dot{W}_{total,before}$	273 MW
Boiler heat from burning fuel	\dot{Q}_b	706.3 MW
Boiler heat input to steam	$\dot{Q}_{th,b}$	614.2 MW
Cycle efficiency	η_{cycle1}	38.65%
Thermal efficiency of the power plant	$\eta_{th,1}$	44.44%
Power plant integrated with solar plant (without LP-turbine extraction)		
Total power output	$\dot{W}_{total,after}$	282.8 MW
Cycle efficiency	η_{cycle2}	40%
Thermal efficiency of the power plant	$\eta_{th,2}$	46%

and from 44% to 46%, respectively. Since economics and levelized cost are the main parameters for evaluating the proposed power plant modification, this marginal increase in efficiencies contributed significantly to saving fuel and emission costs. For example, this 1.4% increase in the cycle efficiency could save 42.9 GWh and 36,480 tons of CO₂ per year from being produced by conventional thermal power plants.

To compare the cost of producing 9.8 MW from different technologies, LCOE analysis has been used. For the steam-powered plant, the LCOE is noticeably much less than Kuwait's cost of electricity generation over the last 25 years, when considering an average crude oil price of \$50/barrel (about seven times). For the PV plant, the input energy rate to the standard solar panel is around 1000 W/m². However, solar panels have an efficiency of 15%–20% at their best for electricity production. Solar polycrystalline panels producing 175 W/m² (assuming an efficiency

of 17.5%) are used in the results. It has been found that the PV plant requires a very high capital cost compared to the conventional plant, but, on the other hand, it requires lower operating and maintenance costs. The resulting LCOE shows a reduction of 21.7% from the conventional power plant to the PV plant, which produces the same 9.8 MW. From the obtained results for the integrated power plant, it can be noted that the capital costs, operating and maintenance costs and LCOE are all less than the steam turbine and PV power plant costs, because the solar plant in this case (Az-Zour South plant) does not require a turbine, storage, or backup. This leads to fewer operating and maintenance costs, as well as extra savings on the fuel because the plant runs entirely on solar power. The optimum aperture area required to produce the 9.8 MW for the PTC solar plant and the LCOE was found to be 25,852 m² and US\$ 0.129/kWh, respectively. These values decreased by 45% and 44%, respectively, compared to the PV plant. This integrating of Az-Zour South power plant with the PTC solar plant decreased the cost of power by 56% compared to a typical steam turbine plant of 9.8 MW power output.

7. Conclusion

This work investigates the effect of hybridizing steam power plant with a PTC solar plant. The governing equations for the power plant data, solar irradiation, and solar plant designs have been modeled using an engineering equation solver software. It was found that replacing the LP turbine extractions from the power plant with a PTC solar plant increased the power output by 9.8 MW without altering other elements of the cycle or boiler load. LCOE analysis was constructed to find the optimum solar area and to compare PTC solar plant with solar photovoltaic (PV) and conventional fossil fuel power plants. LCOE calculations throughout the year revealed that the month of March has the lowest LCOE (US\$ 0.129/kWh) corresponding to an optimum total aperture area of 25,850 m². The results also indicate that the cycle and thermal efficiencies were all improved after hybridizing the power plant by 1.4% and 1.6%. This solar integration of the power plant decreases the cost of power by 56% when compared to a typical steam turbine, which can produce the similar intended power output of 9.8 MW over the 25-year life cycle. The last notable conclusion is the difference between a design based on maximum thermal efficiency and one based on LCOE throughout the life of the project. This difference is explained when calculating the LCOE for each month.

Nomenclature

A	Area (m^2)
C_p	Specific heat of the oil (kJ/kgK)
D	Diameter (m)
F_1, F_R	Efficiency factor, heat removal factor of the collector
G	Radiant energy incident on a surface per unit area (W/m^2)
h	Convection heat transfer coefficient ($W/m^2 K$)
i	Enthalpy (kJ/kg)
K_r, k	Incidence angle modifier, thermal conductivity ($W/m K$)
$LCOE$	Levelized Cost Of Energy ($\$/kWh$)
\dot{m}	Steam mass flow rate (kg/s)
Nu	Nusselt number
P	Pressure (kPa)
\dot{Q}	Heat rate (kW)
Re	Reynolds number
S	Heat absorbed by the receiver (W/m^2)
T	Temperature ($^\circ C$)
U_L	Solar collector heat loss coefficient ($W/m^2 K$)
U_o	Heat loss coefficient ($W/m^2 K$)
ν	Kinematic viscosity of the oil (m^2/s)
V	Velocity (m/s)
\dot{W}	Power output (kW)
W	Width of the solar collector (m)

Subscripts

a	Ambient
b	Boiler
c, cv	Convection, cover
d	Diffuse
g	Ground
m	Mirror
o	Oil
R, r	Radiation, receiver
ri	Receiver inlet
ro	Receiver outlet
t	Total
u	Useful

Greek Symbol

α	Receiver absorptivity
α_t	Tilt angle ($^\circ$)
β	Solar altitude angle ($^\circ$)
γ	Surface solar azimuth ($^\circ$)
γ_i	Intercept factor
δ	Declination angle ($^\circ$)
ε	Emittance
η_r	Optical efficiency
η_{th}	Thermal efficiency
θ	Incidence angle ($^\circ$)
ρ	Reflectivity
σ	Stefan–Boltzmann constant ($5.67 \times 10^{-8} W m^2 K^{-4}$)
τ	Transmittance
φ	Surface azimuth
\emptyset	Solar azimuth angle

Acknowledgment

We gratefully acknowledge the support of Kuwait University.

References

Alotaibi, S., 2011. Energy consumption in Kuwait: Prospects and future approaches. *Energy Policy* 39, 637–643.

- Alsadi, S., Nassar, Y., 2016. Correction of the ASHRAE clear-sky model parameters based on solar radiation measurements in the arabic countries. *Renew. Energy Technol.* 5, 2325–3924, 1–16.
- AREVA, 2016. Solar boost project, end of project report on the Kogan Creek Power Station. Available at: <https://arena.gov.au/assets/2016/09/Kogan-Creek-Solar-Boost-Final-Report.pdf>.
- Baharoon, D.A., Abdul Rahmana, H., Omara, Z.W., Fadhil, S.O., 2015. Historical development of concentrating solar power technologies to generate clean electricity efficiently—A review. *Renew. Sustain. Energy Rev.* 41, 996–1027.
- Bakos, G.C., Tsechelidou, C.h., 2013. Solar aided power generation of a 300 MW lignite-fired power plant combined with line-focus parabolic trough collector's field. *Renew. Energy* 60, 540–547.
- Boukeliaa, T.E., Mecibaha, M.S., Kumarb, B.N., Reddyb, K.S., 2015. Investigation of solar parabolic trough power plants with and without integrated TES (thermal energy storage) and FBS (fuel backup system) using thermic oil and solar salt. *Energy* 88, 292–303.
- Cakici, D.M., Erdogan, A., Colpan, C.O., 2017. Thermodynamic performance assessment of an integrated geothermal powered supercritical regenerative organic Rankine cycle and parabolic trough solar collectors. *Energy* 120, 306–319.
- Clark, J., 1982. An analysis of the technical and economic performance of a parabolic trough concentrator for solar industrial process heat application. *Int. J. Heat Mass Transfer* 25 (9), 1427–1438.
- Duffie, J.A., Beckman, W.A., 2013. *Solar Engineering of Thermal Processes*, fourth ed. John Wiley & Sons, New Jersey.
- Eastman Chemical Company, Technical Data. Therminol VP-1 heat transfer fluid. Available at: <http://ws.eastman.com>.
- Forristall, R., 2003. Heat Transfer Analysis and Modeling of a Parabolic Trough Solar Receiver Implemented in Engineering Equation Solver. National Renewable Energy Laboratory (NREL).
- Fu, R., Chung, D., Lowder, T., Feldman, D., Ardani, K., Margolis, R., 2016. Solar Photovoltaic System Cost Benchmark: Q1 2016. Technical Report NREL/TP-6A20-66532, National Renewable Energy Laboratory (NREL).
- Gaul, H., Rabl, A., 1980. Incidence-angle modifier and average optical efficiency of parabolic trough collectors. *Sol. Energy Eng.* 102, 16–21.
- Haug, M., 2014. Renewables in GCC countries: the next frontier? In: *Future Energy Challenges in the GCC Region*. The Oxford Institute for Energy Studies.
- Kalogirou, S., Lloyd, S., Ward, J., 1997. Modelling, optimization and performance evaluation of a parabolic trough solar collector steam generation system. *Sol. Energy* 60, 49–59.
- Kaushik, S.C., Sairam, A., 2017. Exergy and thermo-economic analyses of solar aided thermal power plants with storage—A Review. *Glob. J. Res. Eng.* 17 (4), Version 1.0. Available at: <https://engineeringresearch.org/index.php/GJRE/article/view/1647>.
- Kurup, P., Turchi, S.C., 2015. Parabolic Trough Collector Cost Update for the System Advisor Model (SAM). Technical Report NREL/TP-6A20-65228, National Renewable Energy Laboratory (NREL).
- Mehrpooya, M., Ashouri, M., Mohammadi, A., 2017. Thermo-economic analysis and optimization of a regenerative two-stage organic Rankine cycle coupled with liquefied natural gas and solar energy. *Energy* 126, 899–914.
- Mills, S., 2017. Combining solar power with coal-fired power plants or cofiring natural gas. In: *IEA Clean Coal Centre*. ISBN: 978-92-9029-602-7.
2017. Ministry of Electricity and Water of Kuwait. Statistical Year Book, Available at: <https://www.mew.gov.kw/Files/AboutUs/Statistics/5/Re/579.pdf>.
- Mokheimer, E.M.A., Dabwan, Y.N., Habib, M.A., Said, S.A.M., Al-Sulaiman, F.A., 2014. Techno-economic performance analysis of parabolic trough collector in Dhahran, Saudi Arabia. *Energy Convers. Manage.* 86, 622–633.
- Padilla, R.V., Demirkaya, G., Goswami, D.Y., Stefanakos, E., Rahman, M., 2011. Heat transfer analysis of parabolic trough solar receiver. *Appl. Energy* 88 (12), 5097–5110.
- Patnode, A.M., 2006. Simulation and Performance Evaluation of Parabolic Trough Solar Power Plants (Master thesis). University of Wisconsin-Madison: College of Engineering.
- Poullikkas, A., Rouvas, C., Hadjipaschalis, I., Kourtis, G., 2012. Optimum sizing of steam turbines for concentrated solar power plants. *Energy Environ.* 3, 9–18.
- Qin, Y., Hu, E., Yongping, Y., Rongrong, Z., 2011. Evaluation of solar aided thermal power generation with various power plants. *Int. J. Energy Res.* 35, 909–922.
- Shahin, M.S., Orhan, M.F., Uygul, F., 2016. Thermodynamic analysis of parabolic trough and heliostat field solar collectors integrated with a Rankine cycle for cogeneration of electricity and heat. *Sol. Energy* 136, 188–191.
- Suojanen, S., Hakkarainen, E., Tähtinen, M., Sihvonen, T., 2017. Modeling and analysis of process configurations for hybrid concentrated solar power and conventional steam power plants. *Energy Convers. Manage.* 134, 327–339.
2014. Worldbank Data: World Development Indicators. IEA Statistics © OECD/IEA, <http://iea.org/stats/index.asp?iea.org/stats/index.asp>.
- You, Y., Hu, E.J., 1999. Thermodynamic advantages of using solar energy in the regenerative Rankine power plant. *Appl. Therm. Eng.* 19, 1173–1180.